Accepted Manuscript

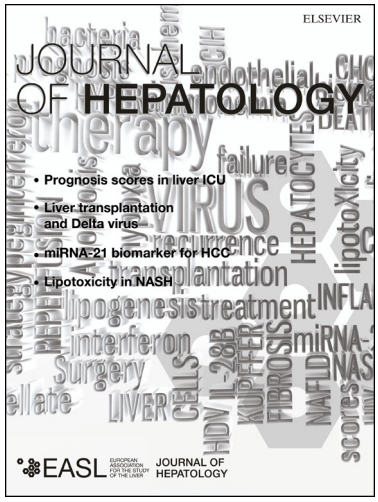

Trail Receptor Deletion in Mice Suppresses the Inflammation of Nutrient Excess

Leila Idrissova, Harmeet Malhi, Nathan W. Werneburg, Nathan K. LeBrasseur, Steve F. Bronk, Christian Fingas, Tamar Tchkonia, Tamar Pirtskhalava, Thomas A. White, Michael B. Stout, Petra Hirsova, Anuradha Krishnan, Christian Liedtke, Christian Trautwein, Niklas Finnberg, Wafik S. El-Deiry, James L. Kirkland, Gregory J. Gores

PII: S0168-8278(14)00882-4
DOI: http://dx.doi.org/10.1016/j.jhep.2014.11.033
Reference: JHEPAT 5454

To appear in: *Journal of Hepatology*

Received Date: 30 June 2014
Revised Date: 14 November 2014
Accepted Date: 18 November 2014

Please cite this article as: Idrissova, L., Malhi, H., Werneburg, N.W., LeBrasseur, N.K., Bronk, S.F., Fingas, C., Tchkonia, T., Pirtskhalava, T., White, T.A., Stout, M.B., Hirsova, P., Krishnan, A., Liedtke, C., Trautwein, C., Finnberg, N., El-Deiry, W.S., Kirkland, J.L., Gores, G.J., Trail Receptor Deletion in Mice Suppresses the Inflammation of Nutrient Excess, *Journal of Hepatology* (2014), doi: http://dx.doi.org/10.1016/j.jhep.2014.11.033

TRAIL RECEPTOR DELETION IN MICE SUPPRESSES THE INFLAMMATION OF NUTRIENT EXCESS

Leila Idrissova[1], Harmeet Malhi[1*], Nathan W. Werneburg[1], Nathan K. LeBrasseur[2], Steve F. Bronk[1], Christian Fingas[1], Tamar Tchkonia[2], Tamar Pirtskhalava[2], Thomas A. White[2], Michael B. Stout[2], Petra Hirsova[1], Anuradha Krishnan[1], Christian Liedtke[3], Christian Trautwein[3], Niklas Finnberg[4], Wafik S. El-Deiry[4], James L. Kirkland[2], Gregory J. Gores[1]

Division of Gastroenterology and Hepatology[1], Robert and Arlene Kogod Center on Aging[2], Mayo Clinic, Rochester, MN 55905; Department of Medicine III, University Hospital[3], Aachen, Germany; Penn State Hershey Cancer Institute[4], Hershey, PA 17033

Address for correspondence: Gregory J. Gores, MD
Professor of Medicine
Mayo Clinic College of Medicine
200 First Street SW
Rochester, Minnesota 55905
Tel: 507 284 0686
Fax: 507 284 0762
E-mail: gores.gregory@mayo.edu

*Co-corresponding author: Harmeet Malhi, MBBS
Assistant Professor of Medicine
Mayo Clinic College of Medicine
200 First Street SW
Rochester, Minnesota 55905
Tel: 507 284 0686
Fax: 507 284 0762
E-mail: malhi.harmeet@mayo.edu

Grant support: This work was supported by NIH grants DK41876 (to GJG), AG13925 and DK50456 (to JLK) DK97178 (to HM), the Deutsche Forschungsgemeinschaft SFB/TRR57 (to CT and CL) and the Mayo Foundation.

Short title: TRAIL Receptor Mediates Metainflammation

Non-standard abbreviations: ALT: alanine aminotransferase, BMDMϕ: bone marrow derived macrophages, CARS: coherent anti-Stokes Raman scattering, C/EBPα: CCAAT/enhancer binding protein (C/EBP) alpha, C/EBPβ: CCAAT/enhancer binding protein (C/EBP) beta, FasL: Fas ligand, FFA: free fatty acid, FFC : fat fructose cholesterol, fMLP: formyl-Methionyl-Leucyl-Phenylalanine, IL1-β: interleukin 1 beta, LPS: lipopolysaccharide, MCP-1: monocyte chemotactic protein-1, NAFLD: nonalcoholic fatty liver disease, NASH: nonalcoholic steatohepatitis, NF-κB: nuclear factor of kappa light polypeptide gene enhancer in B-cells, PA:

palmitate, PCR: polymerase chain reaction, SHG: second-harmonic generation; TNF-α: tumor necrosis factor alpha, TRAIL: TNF-related apoptosis-inducing ligand, TR: TRAIL receptor, TUNEL: terminal deoxynucleotidyl transferase dUTP nick end labeling, WT: wild-type.

Disclosures: The authors report no conflicts

Author Contributions: L.I., N.W.W., S.F.B., C.F., T.T., T.P., T.A.W., M.B.S., P.H., A.K. designed and performed experiments and acquired and analyzed data. N.K.L, C.L., C.T. analyzed and interpreted data, provided material support and contributed to manuscript preparation. N.F., W.S.E., J.L.K. provided material support, analyzed data and contributed to manuscript preparation. L.I., H.M., and G.J.G. conceptualized the study, designed experiments, analyzed and interpreted data and prepared the manuscript.

Total Word Count:	4861
Figures:	4
References:	38
Abstract Word Count:	201

ABSTRACT

Background & Aims: Low-grade chronic inflammation is a cardinal feature of the metabolic syndrome, yet its pathogenesis is not well defined. The purpose of this study was to examine the role of TRAIL receptor (TR) signaling in the pathogenesis of obesity-associated inflammation utilizing mice with the genetic deletion of TR. **Methods**: TR knockout ($TR^{-/-}$) mice and their littermate wild-type (WT) mice were fed a diet high in saturated fat, cholesterol and fructose (FFC) or chow. Metabolic phenotyping, liver injury, and liver and adipose tissue inflammation were assessed. Chemotaxis and activation of mouse bone marrow-derived macrophages (BMDMϕ) was measured. **Results**: Genetic deletion of TR completely repressed weight gain, adiposity and insulin resistance in FFC-fed mice. Moreover, $TR^{-/-}$ mice suppressed steatohepatitis, with essentially normal serum ALT, hepatocyte apoptosis and liver triglyceride accumulation. Gene array data implicated inhibition of macrophage-associated hepatic inflammation in the absence of the TR. In keeping with this, there was diminished accumulation and activation of inflammatory macrophages in liver and adipose tissue. $TR^{-/-}$ BMDMϕ manifest reduced chemotaxis and diminished activation of nuclear factor-κ B signaling upon activation by palmitate and lipopolysaccharide. **Conclusions**: These data advance the concept that macrophage-associated hepatic and adipose tissue inflammation of nutrient excess requires TR signaling.

Keywords: nonalcoholic fatty liver disease, metainflammation, lipoapoptosis, macrophage activation

Chronic low-grade tissue inflammation occurs in obesity-related diseases including type 2 diabetes mellitus and nonalcoholic fatty liver disease (NAFLD). Obesity-associated inflammation appears to be triggered by the recruitment and activation of macrophages within adipose and liver tissues[27]. Inflammation promotes insulin resistance by enhancing lipolysis in adipose tissue and liberating free fatty acids (FFAs) and other lipid mediators into the circulation. Many of these lipids are proinflammatory and can cause cellular demise termed lipotoxicity[30]. For example, elevated concentrations of saturated FFAs cause death of hepatocytes, pancreatic β cells, and adipocytes by apoptosis, a process termed lipoapoptosis[30]. Lipoapoptosis is a histologic hallmark of nonalcoholic steatohepatitis (NASH) and correlates with disease severity[11]. More importantly, the liver contains abundant resident macrophages, Kupffer cells, and their activation or an influx of recruited macrophages has been implicated in the progression of NASH-associated liver injury.[25] Of note, cell death by apoptosis has recently been associated with release of cytokines including monocyte chemotactic protein 1 (MCP-1) which could provide a signal for monocyte recruitment into the liver[8]. Activated macrophages within the tissue may in turn express death ligands such as Fas ligand (FasL), tumor necrosis factor alpha (TNF-α), and TNF-related apoptosis-inducing ligand (TRAIL), further aggravating lipoapoptosis.

Activated macrophages induce inflammation and apoptosis of adjacent cells, in part, by secreting TNF superfamily ligands[32]. Of these ligands, the most potent apoptosis inducers are FasL, TNF-α, and TRAIL. Genetic deletion of Fas protects against adipose tissue inflammation, insulin resistance and hepatic steatosis in mice fed a high fat diet[37]. TNF-α has also been implicated in obesity-associated metabolic syndrome[28]. However, the role of TRAIL and its cognate death receptors in lipotoxicity has not been explored. Yet, several observations implicate

a critical role for TRAIL and/or its cognate receptors in lipotoxicity. TRAIL has been implicated in the genesis of hepatic steatosis[24], and its receptors are upregulated in human NASH specimens[1], dietary models of NASH[10, 14], in genetically obese *ob/ob* mice[18], and in FFA-treated hepatocytes[21]. Serum TRAIL concentrations are associated with anthropometric variables and serum lipids in humans[6], and subcutaneous adipose tissue expression of TRAIL and it's cognate receptors are increased in human obesity[18]. Finally, the saturated FFA palmitate also promotes ligand-independent, TR-initiated hepatocyte cytotoxicity[4]. Thus, the role of TRAIL signaling in obesity-associated inflammation merits further investigation. Mice possess only a single ortholog of the two closely related human TRs (TNFRSF10A and TNFRSF10B).[12],[36] Although the mouse receptor has been referred to as death receptor 5, we have referred to it as TR.

MATERIALS AND METHODS

Animal studies. All animal procedures were approved by the Mayo Clinic Institutional Animal Care and Use Committee. Heterozygotes in a C57BL/6J background were bred to obtain *TR*$^{-/-}$ and wild-type littermate mice as described[12, 36]. Mice were housed 4-5/cage with a 12h light-dark cycle, and *ad libitum* access to food and water. For the dietary studies, the animals were assigned to one of two groups: 1) standard chow diet (Purina LabDiet, St. Louis, MO); or 2) a fructose-fat-cholesterol (FFC) diet (AIN-76A Western Diet 1/2, TestDiet, Richmond, IN) as previously described[5]. This diet provides 40% kcal from fat, 45% kcal from carbohydrate, 15% kcal from protein and has 0.2% cholesterol. Total body weight was measured using a standard balance. Quantitative magnetic resonance was used to quantify lean and fat mass described previously[20]. At the completion of the study, mice were euthanized, blood, liver and adipose tissues were collected[14, 22]. The adipose depots were individually excised and weighed as previously described[29].

Bone marrow derived macrophage isolation and cell migration assays. Bone marrow-derived macrophages (BMDMϕ) were isolated as described[22]. Cell migration assays were performed with BMDMϕ using Corning Transwell plates with 5μm pores (Corning Inc, Corning, NY). BMDMϕ were serum starved for 2 hours, detached with 5 mM EDTA in PBS, and resuspended in RPMI-complete media (RPMI-1640 media with 10% FBS), containing 400 μM PA[4] and/or 10 ng/ml LPS, and applied to the upper chamber. After allowing 1 hour for attachment, TRAIL 100 ng/ml, or fMLP 100 nM were added to the lower chamber. Migration was assessed after an additional 5.5 hours by counting DAPI stained nuclei of migrated and total cells.

Immunofluorescence of p65 NF-κB. BMDMϕ cells were treated with palmitate and/or LPS as above, for 1hour. Cells were fixed with 4% paraformaldehyde, permeabilized with 0.5% Triton X-100 in PBS, blocked with 1% BSA in PBS, and the primary antibody (Santa Cruz Biotechnology, Santa Cruz, CA) was applied overnight at 4°C. Secondary antibody used was Alexa fluor chicken anti-rabbit antisera (Molecular Probes, Eugene, OR) for 1 h at 37°C. Cells were mounted with ProLong antifade with DAPI (Molecular Probes) and images acquired by confocal microscopy (Carl Zeiss, Jena, Germany) with excitation and emission wavelengths of 488 and 507 nm, respectively. Cells with nuclear translocation of p65 NF-κB were quantified and expressed as a percentage of the total cell number.

Immunoblot analysis. Total protein from liver, adipose tissue, and BMDMϕs was isolated, resolved and detected as previously described[22]. Primary antibodies used were: caspase-8 (Enzo Life Sciences, Farmingdale, NY); Ser32/36 IκB-α (Cell Signaling Technology, Danvers, MA); C/EBP-α or C/EBP-β (Santa Cruz Biotechnology). GAPDH (Millipore, Billerica, MA) or β-actin (Santa Cruz Biotechnology) was used as loading control.

ELISA for Monocyte chemotactic protein 1 (MCP-1). MCP-1 was measured in cell culture supernatants of isolated primary hepatocytes with mouse CCL2/JE/MCP-1 DuoSet ELISA Development kit (R&D Systems, Minneapolis, MN) following the manufacturer's instructions. Primary hepatocytes from WT and $TR^{-/-}$ were treated with 400 μM PA for 8h for this assay. The measured MCP-1 concentration was as expressed as pg/ml.

Statistical analysis. Data are presented as mean±SEM except where indicated. Statistical significance between multiple groups was determined by two-tailed ANOVA while statistical difference between two groups was defined by unpaired t-test using GraphPad Prism software. Statistical analysis of the microarray data including gene ontology and pathway analysis

(MetaCore software, Thomson Reuters/Genego, St Joseph, MI and IPA software, Ingenuity Systems, Redwood City, CA) was performed in collaboration with the Division of Biomedical Statistics & Informatics, Mayo Clinic, Rochester, MN.

Supplementary materials and methods. Additional methods including glucose tolerance tests, insulin tolerance tests, indirect calorimetry, adipose tissue characterization, isolation of liver cell subpopulations, RNA isolation, quantitative real-time PCR (qPCR), histologic analyses and biochemical analyses are provided in the supplementary materials and methods section.

RESULTS

***TR*$^{-/-}$ mice are resistant to diet induced obesity.** In accordance with our prior observations[5], mice fed the FFC diet for 6 months weighed significantly more than mice fed standard chow; however, the body weight of wild-type mice was 29% greater than that of *TR*$^{-/-}$ mice (Fig. 1A). *TR*$^{-/-}$ mice had greater relative lean mass and less relative fat mass on the FFC diet compared to wild-type mice (Fig. 1B and C). Chow-fed mice showed no differences between genotypes with regard to total body mass, lean mass or fat mass. Given the reduced fat mass of FFC-fed *TR*$^{-/-}$ mice, we characterized the specific adipose depots. Compared to chow-fed wild-type mice, FFC-fed wild-type animals had larger inguinal, subscapular, epididymal, and mesenteric adipose depots (Fig. 1D); these adipose depots were decreased in size in FFC-fed *TR*$^{-/-}$ mice. Overall, significant visceral fat accumulation occurred in both wild-type and *TR*$^{-/-}$ mice fed the FFC diet compared to respective chow-fed mice; however, this was significantly reduced in FFC-fed *TR*$^{-/-}$ compared to FFC-fed wild-type (Fig. 1E).

To determine whether the protective effects of *TR*$^{-/-}$ on diet-induced obesity were associated with metabolic benefits, we examined glucose tolerance and insulin sensitivity. The 12 hour fasted blood glucose of chow-fed *TR*$^{-/-}$ was lower than wild-type mice (Fig. 1F). The FFC diet caused a significant elevation in fasting blood glucose levels in wild-type mice, but not in *TR*$^{-/-}$ mice, 139.6±5.5 mg/dl and 89.5±7.2 mg/dl, respectively ($p<0.01$). Moreover, following an intraperitoneal bolus of glucose, chow- and FFC-fed *TR*$^{-/-}$ mice had significantly lower glucose concentrations compared to diet-matched wild-type mice. The FFC diet diminished the response of wild-type mice to an exogenous intraperitoneal bolus of insulin (Fig. 1G). In contrast, *TR*$^{-/-}$ mice were protected from diet-induced insulin resistance and displayed preserved insulin sensitivity, comparable to chow-fed *TR*$^{-/-}$ mice. Collectively, these results suggest

deletion of TR confers salutary effects in mice against diet-induced obesity and associated insulin-resistant state. To explain resistance to body weight gain and preserved insulin sensitivity in FFC-fed *TR*$^{-/-}$ mice we looked for differences in caloric intake, physical activity, respiratory exchange ratio and energy expenditure (Supplementary Fig. 1). There were no significant differences in these metabolic parameters between FFC-fed wild-type and FFC-fed *TR*$^{-/-}$ mice. To investigate the tissue injury profiles in these mice, given our interest in the pathogenesis of NASH, and the liver being a key target organ in the metabolic syndrome we first interrogated parameters of liver injury.

Hepatic steatosis and liver injury are reduced in FFC-fed *TR*$^{-/-}$ mice. FFC-fed wild-type mice displayed hepatic steatosis as assessed by histology and CARS microscopy (Fig. 2A and B), increased relative (normalized to body weight) liver weight, (Fig. 2C) hepatic triglyceride content (Fig. 2D), and elevated serum ALT (Fig. 2E) compared to chow-fed mice. In contrast, FFC-fed *TR*$^{-/-}$ mice demonstrated minimal changes in liver histology and no increase in relative liver weight or hepatic triglycerides, and near normal serum ALT. Additional parameters of liver injury, including TUNEL positive apoptotic hepatocytes and hepatic fibrosis assessed by Sirius red staining (Fig. 2F-I) were also increased in FFC-fed wild-type mice. Liver collagen 1 alpha-1 mRNA expression was significantly increased in FFC-fed wild-type mice (Fig. 2J). In contrast, FFC-fed *TR*$^{-/-}$ mice were protected from liver injury and fibrosis much as they were protected from the obese, insulin resistant state. Indeed, a significant reduction in liver triglyceride accumulation, serum ALT elevation, TUNEL positive apoptotic hepatocytes and fibrosis were observed in the FFC-fed *TR*$^{-/-}$ mice. Thus, TR deficiency protected against the hepatic effects of the FFC diet.

Hepatic macrophage infiltration is attenuated in FFC-fed *TR*$^{-/-}$ mice. To define the mechanisms of the hepatoprotective effects of *TR*$^{-/-}$ in an unbiased manner we performed a gene array study in liver tissue from FFC-fed wild-type and *TR*$^{-/-}$ mice. The top ten upregulated and downregulated genes in wild-type mice relative to *TR*$^{-/-}$ mice are reported in Supplementary Table 2. One of the top twenty upregulated genes (26-fold increase) was *Cd68*, a membrane glycoprotein highly expressed by cells of the monocyte/macrophage lineage[23]. Pathway analysis networks also highlighted inflammation-associated genes and networks, especially those associated with phagocytosis (Supplementary Fig. 2). Informed by the gene array data implicating inflammation due to cells of the monocyte/macrophage lineage in this model of steatohepatitis, we next focused on the role of TR in macrophage biology during obesity-associated inflammation.

The substantial accumulation of hepatic macrophages in FFC-fed wild-type mice compared to *TR*$^{-/-}$ mice was confirmed by Mac-2 immunohistochemistry, a phenotypic marker for phagocytically active macrophages[17] (Fig. 3A). We saw exuberant macrophage accumulation around fatty hepatocytes in FFC-fed wild-type mice, consistent with the literature [31]. In addition, qPCR for macrophage markers, *Cd68* (Fig. 3B) and *F4/80* (Fig. 3C) was consistent with the histology, demonstrating a significant increase in these markers in FFC-fed wild-type mice. In contrast, these macrophage markers were significantly reduced in FFC-fed *TR*$^{-/-}$ mice compared to diet-matched wild-type mice. The accumulation of macrophages was accompanied by increased proinflammatory cytokine response in FFC-fed wild-type mice as assessed by measurement of *Mcp1* (Fig. 3D) and *Tnfα* (Fig. 3E). In marked contrast, *Tnfα* and *Mcp1* mRNA levels were substantially reduced in FFC-fed *TR*$^{-/-}$ mice. Correspondingly, *Cd11c*

and *Ly6c,* markers of monocyte-derived macrophages, known to be proinflammatory, were significantly upregulated in FFC-fed wild-type mice compared to *TR*$^{-/-}$ mice (Fig. 3F and G).

Hepatocyte and macrophage TR signaling is upregulated and contributes to the inflammation of nutrient excess. To further examine the role of TR signaling in our model, we quantified *Trail* and *TR* mRNA expression in liver from FFC-fed and chow-fed mice and found an increase in both in liver (Supplementary Fig. 3A and B). Next, we used a cell fractionation approach to define the cellular source of increased hepatic *Trail* and *TR* expression, and found that the FFC diet increased *Trail* mRNA abundance in hepatocytes and *TR* mRNA abundance in macrophages and hepatocytes (Supplementary Fig. 3C and E). These data suggest TR signaling in two cell types, hepatocytes and macrophages, contributes to tissue inflammation in this model. Given, the existing data on lipotoxic ligand-independent activation of TR signaling in fatty hepatocytes leading to lipoapoptosis [4], we further explored TR signaling in macrophages.

TR signaling in BMDMϕ promotes macrophage chemotaxis and activation. We first examined a role for TR signaling in macrophage chemotaxis and activation. *TR*$^{-/-}$ and wild-type BMDMϕ migrated equally to fMLP; however *TR*$^{-/-}$ BMDMϕ demonstrated reduced migration to TRAIL (Fig. 4A and B). Thus, TRAIL was a chemoattractant for macrophages consistent with our observations of enhanced macrophage accumulation in FFC-fed wild-type mice. Due to the enhanced liver injury and inflammation in FFC-fed wild-type mice, and its significant abrogation in *TR*$^{-/-}$ mice, we next explored if TRAIL signaling is proinflammatory in macrophages, in addition to its chemotaxis effects. We treated macrophages with palmitate, a known proinflammatory saturated fatty acid implicated in lipotoxicity, alone or in combination with low dose lipopolysaccharide (LPS)[34]. Palmitate and LPS induced *Tnfα*, *Il1β* and *Mcp1*, in wild-type, but not *TR*$^{-/-}$ hepatic macrophages (Fig. 4C-E). As hepatocyte apoptosis is associated with

chemokine production,[8] we measured MCP-1 in cell culture supernatants of hepatocytes from wild-type and *TR*$^{-/-}$ mice treated with palmitate. Treatment with palmitate induced MCP-1 secretion in wild-type hepatocytes, but not in *TR*$^{-/-}$ cells (Fig. 4F). This correlates with the increased hepatocyte apoptosis and increased MCP-1 abundance seen in FFC-fed wild-type versus *TR*$^{-/-}$ mice, suggesting that chemokines from injured hepatocytes recruit inflammatory macrophages to the liver. Furthermore, *TR*$^{-/-}$ macrophages demonstrate reduced chemotaxis and activation under lipotoxic conditions.

To define the mechanisms of diminished recruitment of *TR*$^{-/-}$ BMDMϕ into the liver of FFC-fed mice we explored NF-κB signaling, a nonapoptotic signaling pathway activated by TRAIL and its cognate receptors[3]. *TR*$^{-/-}$ BMDMϕ manifest reduced p65 NF-κB subunit nuclear translocation when stimulated with a combination of palmitate plus LPS compared to wild-type cells (Fig. 4G and H). Because palmitate can induce TR signaling by a ligand-independent mechanism[4], we postulated that TRAIL could substitute for palmitate in this assay. Indeed, TRAIL plus LPS yielded similar results for p65 NF-κB subunit nuclear translocation to palmitate plus LPS. We confirmed NF-κB activation by examining IκB-α phosphorylation. Palmitate plus LPS induced a substantial increase in IκB-α (Ser32/36) phosphorylation (Fig. 4H). In contrast, IκB-α (Ser32/36) phosphorylation was significantly reduced in *TR*$^{-/-}$ cells. Similar to the nuclear translocation studies, TRAIL substitutes for palmitate in this assay. Thus, *TR*$^{-/-}$ BMDMϕ display reduced levels of NF-κB activation in response to palmitate plus LPS or TRAIL plus LPS stimulation. This likely contributes to the reduced activation of macrophages *in vivo* in FFC-fed mice. Having demonstrated a reduction in hepatic injury and inflammation in FFC-fed TR-/- mice, and reduced chemotaxis and activation

in TR-/- macrophages, we next turned our attention to the expanded white adipose tissue to examine its role in the improved metabolic phenotype on *TR*$^{-/-}$ mice.

***TR*$^{-/-}$ mice exhibit decreased adiposity and adipose tissue inflammation.** FFC feeding led to adipocyte expansion. H&E stained adipose tissue is shown in supplementary figure 4A. This was quantified by measuring adipocyte diameter in epididymal and inguinal fat pads; these fat pads demonstrated larger adipocytes with increased adipocyte diameter in FFC-fed wild-type mice as compared to chow-fed mice; however, adipocyte diameter in FFC-fed *TR*$^{-/-}$ mice was comparable to chow-fed mice (Supplementary Fig. 4B and C). As adipose tissue expansion is governed, in part, by master transcriptional regulators C/EBPα and β[19], we examined their expression by mRNA and immunoblot analysis. As anticipated, C/EBPα and β were both upregulated in FFC-fed wild-type mice (Supplementary Fig. 4D-G). In contrast, but likely contributing to the lack of adipose tissue expansion in FFC-fed *TR*$^{-/-}$, we observed lower levels of C/EBPα and C/EBPβ.

To further characterize features of the expanded adipose tissue, we asked if development of beige or brown fat-like properties might account for the reduction in adipose tissue expansion in FFC-fed *TR*$^{-/-}$ mice. We observed no increase in markers of beige fat in adipose tissue from FFC-fed wild-type or *TR*$^{-/-}$ mice (Supplementary Fig. 4H and I). However, we detected a trend towards increased uncoupling protein-1 (UCP-1) mRNA expression in *TR*$^{-/-}$ mice (Supplementary Fig. 4K). Although there was not a statistically significant difference, this trend towards enhanced UCP-1expression in the *TR*$^{-/-}$ mice, perhaps explains, in part, their improved metabolic phenotype. Correspondingly, we detected an increase in UCP-1 by immunohistochemistry in *TR*$^{-/-}$ mice (Supplementary Fig. 4L). We confirmed that the UCP1 antibody worked in our hands by testing it on brown adipose tissue (Supplementary Fig. 6). The

immunohistochemistry for UCP-1 identifies a pattern of adipose tissue browning associated with fibroblast-like cells within the tissue, which may account for the improved metabolic phenotype in the *TR*$^{-/-}$ mice [2]. Lastly, we analyzed characteristics of infiltrating macrophages in adipose tissues. First, we found an increase in TR expression in FFC-fed wild-type mice without a corresponding increase in adipose tissue TRAIL (Supplementary Fig. 5A and B). There was a significant increase in *Cd68* and *F4/80* consistent with macrophage accumulation and *Tnf*α and *Mcp1* mRNA abundance in FFC-fed wild-type white adipose tissues (Supplementary Fig. 5C-F), supporting the accumulation of pro-inflammatory macrophages in FFC-fed wild-type mice, and a significant reduction in the accumulation of pro-inflammatory macrophages in white adipose tissue in FFC-fed *TR*$^{-/-}$ mice. We did not detect an increase in alternatively activated, M2 macrophages in FFC-fed white adipose tissue (Supplementary Fig. 5G-I). Thus, consistent with the observations in liver tissue, we found increased pro-inflammatory macrophages in adipose tissue of FFC-fed obese mice.

DISCUSSION

The current observations provide key mechanistic insights into the signaling pathways that form the basis of the inflammation of dietary nutrient excess. We observed, in a murine model of obesity and insulin resistance, genetic deletion of TR provided several salutary effects including: i) protection against an increase in adiposity and insulin resistance; ii) reduction in steatohepatitis; iii) suppression of accumulation of pro-inflammatory macrophages in the liver; and iv) reduction in adipose tissue pro-inflammatory macrophage accumulation. *In vitro*, the genetic deletion of TR attenuated macrophage activation responses following co-stimulation with palmitate plus LPS. These data implicate TR signaling as a potent process in the inflammatory response occurring during nutrient excess.

We employed the FFC diet to mimic a fast food diet and obtain a model of obesity with steatohepatitis, which mimics human NASH[5]. Genetic deletion of the TR attenuates many of the adverse metabolic features observed in wild-type mice fed this diet. Interestingly, $TR^{-/-}$ mice have reduced body mass, reduced steatohepatitis, reduced macrophage accumulation in liver and adipose tissues in spite of equal energy intake and expenditure. These observations suggest TR signaling plays a pivotal role in initiating the inflammatory response to nutrient excess. Without an inflammatory response, insulin resistance, weight gain, and organ lipotoxicity are attenuated, highlighting the role of inflammation in the pathogenesis of the metabolic syndrome[26].

During nutrient excess the resulting surplus of circulating FFAs are extracted by the liver with adverse outcomes, namely lipoapoptosis[30]. This hepatocyte lipoapoptosis is, in part, mediated by TR signaling *in vitro*[4]. Our current data extends these concepts by demonstrating reduced steatohepatitis in FFC-fed animals with TR deletion. Consistent with our observations, it has been demonstrated that apoptosis resistant mice due to hepatocyte-specific deletion of

caspase 8 also have reduced hepatocyte apoptosis and consequently reduced steatohepatitis when fed a methionine and choline deficient diet[13]. Proapoptotic TR signaling in hepatocytes likely elicits an inflammatory response activating macrophages and promoting the development of steatohepatitis[8]. Thus, inhibition of TR proapoptotic signaling may prevent inflammation and insulin resistance simply by attenuating cell death in the liver and other tissues, as has been demonstrated with pharmacologic caspase inhibition[35]. Alternatively, due to the improved metabolic profile of FFC-fed $TR^{-/-}$ mice, and the associated reduction in inflammation, we cannot exclude a reduction in hepatocyte lipoapoptosis occurring secondary to a better metabolic profile. Due to the whole body knockout mouse employed in these studies the tissue- and organ-specific roles cannot be teased out; however, we hope to address this in the future with tissue-specific $TR^{-/-}$ mice.

Although absence of cell death may be sufficient to prevent inflammation, death receptors also exert proinflammatory signaling cascades in multiple cell types[3]. Indeed, palmitate treatment of primary mouse hepatocytes resulted in MCP-1 generation, similar to Fas[8]. As palmitate plus LPS triggers secretion of proinflammatory cytokines in cells of the monocyte lineage[34], we employed these mediators in our study of macrophages. Interestingly, enhanced expression of *Mcp-1*, *Tnfα*, and *Il1β* by LPS plus palmitate was suppressed in $TR^{-/-}$ hepatic macrophages and BMDMϕ. This observation is likely explained by the decrease in canonical NF-κB activation in $TR^{-/-}$ cells. Both TR signaling, and LPS signaling *via* Toll-like receptor 4 (TLR4), can engage TRAF6 as a platform to activate NF-κB[15, 38]. Perhaps overlap in this signaling process results in synergy between palmitate induced TR signaling plus LPS-mediated TLR4 signaling. This latter testable concept will require further studies to identify how

TR non-apoptotic signaling synergizes with LPS stimulation to activate pro-inflammatory NF-κB signaling in macrophages.

Our studies demonstrate an increase in TR expression in FFC-fed wild-type white adipose tissue, and an increase in both TRAIL and TR in FFC-fed wild-type livers, suggesting that TR signaling in both liver and adipose tissue may play a role in the pathogenesis of obesity associated tissue injury. Indeed, in FFC-fed *TR*$^{-/-}$ mice a reduction in adipose depots, fat mass, and adipocyte size was observed. In addition, we show that the induction of master regulators of adipogenic expansion is impaired in FFC-fed *TR*$^{-/-}$ mice suggesting that TR signaling is required for maximal adipose expansion under FFC feeding conditions. An increase in brown fat-like features of adipose tissue, characterized by fibroblast-like cells within the tissue, was detected in *TR*$^{-/-}$ mice, which may account for the improved metabolic phenotype in the *TR*$^{-/-}$ mice. Our data suggest that TR signaling is essential for the development of diet-induced obesity and its sequelae, and its deletion limits both lipoapoptosis and tissue inflammation.

One unifying explanation for these findings could be a primary macrophage defect, as the current study suggests that TR signaling contributes to the immune response of nutrient excess by promoting macrophage chemotaxis and the inflammatory response to FFAs. Thus, due to the lack of macrophage accumulation and activation in both adipose tissue and liver, *TR*$^{-/-}$ mice are protected from insulin resistance and the progressive deleterious effects of diet-induced obesity. The pathophysiology of TRAIL and its receptors has remained somewhat enigmatic. TRAIL signaling was originally identified as proapoptotic in malignant cell lines but was uneventful in healthy, nontransformed cells[16]. Recently, a role for non-apoptotic TR signaling in host immune responses has emerged[3, 9]. Our findings are in accord with this growing appreciation of the role of TR in inflammatory disorders[7].

We propose a model where TR signaling, by promoting both cell death and macrophage activation, results in tissue inflammation and insulin resistance during dietary nutrient excess. Both processes coordinately participate in the observed phenotype. Finally, we note that a small molecule TR agonist has been described, which suggests that identifying a small molecule TR antagonist is also possible[33]. An inhibitor of TR signaling could be salutary in human obesity related syndromes if the observations in mice can be extrapolated to humans.

ACKNOWLEDGEMENTS

We thank Ms. Courtney Hoover for outstanding secretarial assistance.

REFERENCES

[1] Affo S, Dominguez M, Lozano JJ, Sancho-Bru P, Rodrigo-Torres D, Morales-Ibanez O, et al. Transcriptome analysis identifies TNF superfamily receptors as potential therapeutic targets in alcoholic hepatitis. Gut 2012.
[2] Asterholm IW, Scherer PE. Enhanced metabolic flexibility associated with elevated adiponectin levels. Am J Pathol 2010;176(3): 1364-1376.
[3] Benedict CA, Ware CF. TRAIL: not just for tumors anymore? J Exp Med 2012;209(11): 1903-1906.
[4] Cazanave SC, Mott JL, Bronk SF, Werneburg NW, Fingas CD, Meng XW, et al. Death receptor 5 signaling promotes hepatocyte lipoapoptosis. J Biol Chem 2011;286(45): 39336-39348.
[5] Charlton M, Krishnan A, Viker K, Sanderson S, Cazanave S, McConico A, et al. Fast food diet mouse: novel small animal model of NASH with ballooning, progressive fibrosis, and high physiological fidelity to the human condition. American journal of physiology Gastrointestinal and liver physiology 2011;301(5): G825-834.
[6] Choi JW, Song JS, Pai SH. Associations of serum TRAIL concentrations, anthropometric variables, and serum lipid parameters in healthy adults. Ann Clin Lab Sci 2004;34(4): 400-404.
[7] Collison A, Foster PS, Mattes J. Emerging role of tumour necrosis factor-related apoptosis-inducing ligand (TRAIL) as a key regulator of inflammatory responses. Clin Exp Pharmacol Physiol 2009;36(11): 1049-1053.
[8] Cullen SP, Henry CM, Kearney CJ, Logue SE, Feoktistova M, Tynan GA, et al. Fas/CD95-Induced Chemokines Can Serve as "Find-Me" Signals for Apoptotic Cells. Mol Cell 2013.
[9] Diehl GE, Yue HH, Hsieh K, Kuang AA, Ho M, Morici LA, et al. TRAIL-R as a negative regulator of innate immune cell responses. Immunity 2004;21(6): 877-889.
[10] Farrell GC, Larter CZ, Hou JY, Zhang RH, Yeh MM, Williams J, et al. Apoptosis in experimental NASH is associated with p53 activation and TRAIL receptor expression. Journal of gastroenterology and hepatology 2009;24(3): 443-452.
[11] Feldstein AE, Canbay A, Angulo P, Taniai M, Burgart LJ, Lindor KD, et al. Hepatocyte apoptosis and fas expression are prominent features of human nonalcoholic steatohepatitis. Gastroenterology 2003;125(2): 437-443.
[12] Finnberg N, Gruber JJ, Fei P, Rudolph D, Bric A, Kim SH, et al. DR5 knockout mice are compromised in radiation-induced apoptosis. Molecular and cellular biology 2005;25(5): 2000-2013.
[13] Hatting M, Zhao G, Schumacher F, Sellge G, Masaoudi MA, Gabetaler N, et al. Hepatocyte caspase-8 is an essential modulator of steatohepatitis in mice. Hepatology 2013.
[14] Hirsova P, Ibrahim SH, Bronk SF, Yagita H, Gores GJ. Vismodegib Suppresses TRAIL-mediated Liver Injury in a Mouse Model of Nonalcoholic Steatohepatitis. PLoS One 2013;8(7): e70599.
[15] Inoue J, Gohda J, Akiyama T. Characteristics and biological functions of TRAF6. Adv Exp Med Biol 2007;597: 72-79.
[16] Johnstone RW, Frew AJ, Smyth MJ. The TRAIL apoptotic pathway in cancer onset, progression and therapy. Nat Rev Cancer 2008;8(10): 782-798.

[17] Jordan SD, Kruger M, Willmes DM, Redemann N, Wunderlich FT, Bronneke HS, et al. Obesity-induced overexpression of miRNA-143 inhibits insulin-stimulated AKT activation and impairs glucose metabolism. Nat Cell Biol 2011;13(4): 434-446.
[18] Keuper M, Wernstedt Asterholm I, Scherer PE, Westhoff MA, Moller P, Debatin KM, et al. TRAIL (TNF-related apoptosis-inducing ligand) regulates adipocyte metabolism by caspase-mediated cleavage of PPARgamma. Cell Death Dis 2013;4: e474.
[19] Lefterova MI, Lazar MA. New developments in adipogenesis. Trends Endocrinol Metab 2009;20(3): 107-114.
[20] Liu L, Brown D, McKee M, Lebrasseur NK, Yang D, Albrecht KH, et al. Deletion of Cavin/PTRF causes global loss of caveolae, dyslipidemia, and glucose intolerance. Cell Metab 2008;8(4): 310-317.
[21] Malhi H, Barreyro FJ, Isomoto H, Bronk SF, Gores GJ. Free fatty acids sensitise hepatocytes to TRAIL mediated cytotoxicity. Gut 2007;56(8): 1124-1131.
[22] Malhi H, Kropp EM, Clavo VF, Kobrossi CR, Han J, Mauer AS, et al. C/EBP homologous protein-induced macrophage apoptosis protects mice from steatohepatitis. J Biol Chem 2013;288(26): 18624-18642.
[23] Miura K, Yang L, van Rooijen N, Ohnishi H, Seki E. Hepatic recruitment of macrophages promotes nonalcoholic steatohepatitis through CCR2. American journal of physiology Gastrointestinal and liver physiology 2012;302(11): G1310-1321.
[24] Mundt B, Wirth T, Zender L, Waltemathe M, Trautwein C, Manns MP, et al. Tumour necrosis factor related apoptosis inducing ligand (TRAIL) induces hepatic steatosis in viral hepatitis and after alcohol intake. Gut 2005;54(11): 1590-1596.
[25] Obstfeld AE, Sugaru E, Thearle M, Francisco AM, Gayet C, Ginsberg HN, et al. C-C chemokine receptor 2 (CCR2) regulates the hepatic recruitment of myeloid cells that promote obesity-induced hepatic steatosis. Diabetes 2010;59(4): 916-925.
[26] Odegaard JI, Chawla A. Pleiotropic actions of insulin resistance and inflammation in metabolic homeostasis. Science 2013;339(6116): 172-177.
[27] Oh DY, Morinaga H, Talukdar S, Bae EJ, Olefsky JM. Increased macrophage migration into adipose tissue in obese mice. Diabetes 2012;61(2): 346-354.
[28] Shoelson SE, Herrero L, Naaz A. Obesity, inflammation, and insulin resistance. Gastroenterology 2007;132(6): 2169-2180.
[29] Tchkonia T, Thomou T, Zhu Y, Karagiannides I, Pothoulakis C, Jensen MD, et al. Mechanisms and metabolic implications of regional differences among fat depots. Cell Metab 2013;17(5): 644-656.
[30] Unger RH, Clark GO, Scherer PE, Orci L. Lipid homeostasis, lipotoxicity and the metabolic syndrome. Biochim Biophys Acta 2010;1801(3): 209-214.
[31] Van Rooyen DM, Gan LT, Yeh MM, Haigh WG, Larter CZ, Ioannou G, et al. Pharmacological cholesterol lowering reverses fibrotic NASH in obese, diabetic mice with metabolic syndrome. J Hepatol 2013;59(1): 144-152.
[32] Vujanovic NL. Role of TNF superfamily ligands in innate immunity. Immunol Res 2011;50(2-3): 159-174.
[33] Wang G, Wang X, Yu H, Wei S, Williams N, Holmes DL, et al. Small-molecule activation of the TRAIL receptor DR5 in human cancer cells. Nat Chem Biol 2013;9(2): 84-89.
[34] Wen H, Gris D, Lei Y, Jha S, Zhang L, Huang MT, et al. Fatty acid-induced NLRP3-ASC inflammasome activation interferes with insulin signaling. Nat Immunol 2011;12(5): 408-415.

[35] Witek RP, Stone WC, Karaca FG, Syn WK, Pereira TA, Agboola KM, et al. Pan-caspase inhibitor VX-166 reduces fibrosis in an animal model of nonalcoholic steatohepatitis. Hepatology 2009;50(5): 1421-1430.
[36] Wu GS, Burns TF, Zhan Y, Alnemri ES, El-Deiry WS. Molecular cloning and functional analysis of the mouse homologue of the KILLER/DR5 tumor necrosis factor-related apoptosis-inducing ligand (TRAIL) death receptor. Cancer Res 1999;59(12): 2770-2775.
[37] Wueest S, Rapold RA, Schumann DM, Rytka JM, Schildknecht A, Nov O, et al. Deletion of Fas in adipocytes relieves adipose tissue inflammation and hepatic manifestations of obesity in mice. J Clin Invest 2010;120(1): 191-202.
[38] Yen ML, Hsu PN, Liao HJ, Lee BH, Tsai HF. TRAF-6 dependent signaling pathway is essential for TNF-related apoptosis-inducing ligand (TRAIL) induces osteoclast differentiation. PLoS One 2012;7(6): e38048.

FIGURE LEGENDS

Fig. 1. *TR*$^{-/-}$ mice are resistant to diet induced obesity. (A) Body weight in grams (g), (B) Lean mass (%), (C) Fat mass (%), (D) White adipose tissue (g), (E) Visceral fat (%), (F) Serum glucose determinations following an intraperitoneal injection of glucose, and (G) Serum glucose determinations following an intraperitoneal injection of insulin in wild-type (WT) and TR knockout (*TR*$^{-/-}$) mice fed chow or FFC diet for 6 months (n=7 per group). For B and C the percent lean and fat mass totals to approximately 90%, as QMR excludes skin and bones which accounts for the remaining 10% body mass. For A-E *p<0.05, **p<0.01. For F and G the differences between FFC-fed WT versus *TR*$^{-/-}$ mice are statistically significant by two-tailed ANOVA (*p<0.05).

Fig. 2. Hepatic steatosis and liver injury are reduced in FFC-fed *TR*$^{-/-}$ mice. (A) H&E stained sections (scale bar 20 μm), (B) CARS and SHG microscopy for lipid droplets and extracellular matrix (scale bar 100 μm), (C) Liver weight, (D) Hepatic triglycerides (μg/mg of liver tissue), (E) Serum alanine aminotransferase (U/L), (F) TUNEL staining (scale bar 100 μm), (G) Sirius red staining (scale bar 100 μm), (H) Quantification of TUNEL positive cells, (I) Quantification of Sirius red chromogen, and (J) mRNA abundance of collagen-1α1 in livers from WT and *TR*$^{-/-}$ mice fed chow or FFC diet for 6 months (n=7/group). *p<0.05, **p<0.01.

Fig. 3. Liver and adipose tissue macrophage infiltration is attenuated in FFC-fed *TR*$^{-/-}$ mice. (A) Liver section with Mac-2 immunohistochemistry for macrophages (scale bar 20 μm), mRNA abundance of (B) *Cd68*, (C) *F4/80*, (D) *Mcp1*, (E) *Tnfα*, (F) *Cd11c* and (G) *Ly6c* in liver tissue, (H) *Cd68*, (I) *F4/80*, (J) *Tnfα* and (K) *Mcp1* in epididymal fat of WT and *TR*$^{-/-}$ mice fed the FFC diet for 6 months expressed relative to that observed in chow-fed WT mice (n=6 per group, *p<0.05, **p<0.01).

Fig. 4. Macrophage TR signaling contributes to the inflammation of nutrient excess.

(A) Fluorescent photomicrographs (scale bar 20 μm) and (B) quantification of DAPI stained migrated WT and *TR*$^{-/-}$ BMDMϕ. (C-E) mRNA abundance of *Tnfα, Il1β,* and *Mcp1* in cells treated with 400 μM palmitate (PA) and/or 10 ng/ml lipopolysaccharide (LPS), 8h. (F) MCP1 levels in supernatants from cells treated with 400 μM PA, 8h. (G) Quantification of nuclear translocation of NF-κB by immunofluorescence, (H) phosphorylation of IκB-α (Ser32/Ser36) in WT and *TR*$^{-/-}$ BMDMϕ treated with 400 μM PA ± 10 ng/ml lipopolysaccharide (LPS) or 10 ng/ml TRAIL for 1h. *$p<0.05$, **$p<0.01$